ISSN: 2994-7510

Research Article

Journal of Water Research

Evaluating the Impact of Climate Change on Crop Water Requirements for Rainfed Agriculture in Ethiopia

Zablon Adane[1*], Tinebeb Yohannes[1] and Paolo Nasta[2]

[1]*World Resources Institute, Washington DC, 20002*

[2]*Department of Agriculture, Division of Agricultural, Forest and Biosystems Engineering*

[*]Corresponding Author
Zablon Adane, World Resources Institute, Washington DC, 20002.

Submitted: 2024, Dec 01; **Accepted:** 2024, Dec 26; **Published:** 2025, Jan 08

Citation: Adane, Z., Yohannes, T., Nasta, P. (2025). Evaluating the Impact of Climate Change on Crop Water Requirements for Rainfed Agriculture in Ethiopia. *J Water Res, 3*(1), 01-21.

Abstract
Rainfed agriculture in Ethiopia is critical for food security and the national economy. Ethiopia naturally experiences high climate variability, which has historically exposed its rainfed agriculture to severe dry shocks. Climate change stands to exacerbate this challenge and intensify vulnerability. Therefore, it is essential to evaluate the impact of climate change on all crops in Ethiopia. In this study, the crop water requirement (CWR) was used as a proxy to water stress. An ensemble modeling based on HYDRUS-1D was used to evaluate the impact of climate change on CWR for 36 crops in Ethiopia. The analysis explores the response of mean annual CWR to the historical climate and dry, most probable, and wet climate projections, prioritized based on Aridity Index (AI). The three models at a national level predict wetter-than-normal conditions, however, detecting critical hotspots where drier conditions may increase crop-specific drought stress is important. A non-linear decay in CWR was detected as a function of historical and projected AI. Sensitivity of CWR to changes in AI identified the most vulnerable hotspots to drought for perennial crops while weak sensitivity was observed in annual crops. This analytical study will be instrumental in detecting vulnerable crops to climate change, explore areas of intervention, and identify potential deep-dives. The reliance on global datasets and the use of one-dimensional hydrological model represent the main limitations of this study.

Keywords: Ensemble Modeling Approach, Food Security, Aridity Index, HYDRUS-1D, Drought Sensitivity, Rainfed Agriculture, Crop Water Requirement

1. Introduction

Ethiopia is heavily dependent on agriculture for the overall economy, livelihoods, and food security. Agriculture accounts for nearly 40% of the Ethiopian gross domestic product (GDP), 90% of exports, and approximately 66% of employment in 2020 [1,2]. Approximately 80% of Ethiopians live in rural areas and mostly rely on rainfed agriculture for their livelihoods.

The national average landholding per household in 2012 was just 1.15ha with the Southern Nations Nationalities People Region accounting for the least average landholding at less than 0.5 ha per household [3]. The population of Ethiopia has more than doubled since the 1970s from 55 million in 1970 to 117 million in 2020 and is expected to double to more than 200 million by 2050 putting further constrictions in landholding and livelihoods [4]. Low productivity and growing population pressures have created the conditions for internal strife and conflict, serious internal displacement often to already densely populated cities, and illegal migration to Europe and North America through extremely dangerous means and pathways.

Food security in Ethiopia is a critical concern due to high rainfall variability both in time and space, small landholding per household, degraded lands and poor land management practices,limited agricultural input, and the subsistence nature of farming across the country [5-9]. While rainfed agriculture is estimated to be approximately 20 million ha of land, irrigation only accounts for around 1 million ha (~5%) of current farmland. Grain crop yields from smallholder farmlands (2.8 tons per ha) on average are well below the global (4 ton per ha) and high-income country (8 tons per ha) averages [10,11]In addition, market supply chain development is in its infancy and applications of improved seed varieties, fertilizer input, and pesticides remain limited.

Ethiopian farmers and producers heavily rely on rainfed agriculture, which is highly susceptible to climate change [12]. Vulnerability to climate in Ethiopia is often associated with high rainfall variability including change in the timing and intensity of precipitation. The impact of climate change on crop yield can include water stress, seasonal shift resulting in altered planting times and length of growing period, which may require increased water storage capacity, crop shifting, and other adaptation mechanisms.

The climate has been historically highly variable across the country and will likely remain variable through time. Climate projections indicate that climate change will cause a slight decrease to an increase in precipitation (FDRE MoFED) while others also suggest seasonal shifts in precipitation and more intense rainfall in humid parts of Ethiopia. While there is no consensus in rainfall projections, models consistently predict an increase in temperature including a rise in average temperature by 1.3 ^{o}C since 1960 [13].

An increase in temperature induces an increase in atmospheric demand and incrop evapotranspiration. A shift in precipitation pattern, magnitude, and intensity will also impact availability of water for crops during the growing period, increase likelihood of water surplus stress (floods) and water deficit stress (droughts), which can lead to root water stress and potential crop failures.

Progress in yield related to increased cultivated area for cereals has been considerable over past decades [14]. However, productivity measured by yield per hectare is still markedly low compared to global averages and highly susceptible to dry shocks. Thus, improving production levels and reducing vulnerability to climate shocks are essential components to enhance food security in Ethiopia in terms of sufficient food availability and securing rural livelihoods. While climate change and rainfall variability impacts are directly related to water availability for crops, crop productivity and yield also rely on other factors including soil fertility, agricultural inputs such as fertilizer and pesticides, and suitable land management and agricultural practices.

Efforts focusing on the impact of climate change on water supply in Ethiopia are plethora [15]. Similarly, efforts exploring rainfed agriculture in Ethiopia are equally ubiquitous. However, despite the importance of understanding the impact of climate change on rainfed agriculture and the need for adaptation and mitigation measures for food security across the country, the existing body of work on climate change and rainfed agricultural and development in Ethiopia has mostly focused on specific crop types and in narrow geographic areas [16,17].

This study instead will explore the complete list of dominant crop types currently present in Ethiopia and evaluate the impact of climate change on water availability for rainfed agriculture over the entire country. This initial broad analysis can help identify both the crop type and specific geographic locations that require greater attention for food security concerns amid climate change and further support deep dive analyses of targeted research as well as policy development for climate adaptation and resilience.

The objective of this paper is two-fold. First, compare the observed historical time serieswith the climate change scenarios in terms of rainfall andtemperature-based reference evapotranspiration. The FAO aridity index, AI is used as climate descriptor and identify extremely dry, most probable, and extremely wet climate projections [18]. Second, understand the impact of climate change on crop water requirement of the main 36 crops in the agro-ecological zones of Ethiopia.

2. Materials and Methods

2.1 Study Area

Ethiopia is a landlocked country located in the Horn of Africa and extends from 15 N 3N to 33E 48E (Figure 1). It is the second most populous (120 million) and second largest country with approximately 1.1 million km^2 land coverage in Africa. The landscape ranges from lowlands to highlands and ranges from –125 m in the Afar Region (the Dalol Depression in the northeastern Lowlands) to 4,550 m (Mount Ras Dashen in the northern Highlands). TheEast African Rift Valley crosses the country on a northeast-southwest axis [19].

The climate ranges from arid in the southeastern part to humid, sub-humid, and tropical in most parts of Ethiopia. While the annual rainfall average is approximately 850 mm per year, it is variable over space and time with the dry and wet parts of the country receiving as low as 300 mm and more than 2000 mm per year, respectively [11]. Rainfall amounts are characterized bytwo rainy seasons namelyBelg (February to May)andKiremt (June to September). Most of the annual rainfall occurs in the Kiremt season. The dry season known as Bega occurs between October and January. Ethiopia has 12 river basins (8 are wet and 4 are relatively dry), of which the western part of the country accounts for 70% of the total river flow [20].

The agricultural land coverage in Ethiopia is approximately 94% rainfed with 20 million ha and 6% irrigated land (Figure 1). Land uses in Ethiopia include cropland, forest, grassland, shrubland, water bodies (Figure 2a).Similarly, the agro-ecological zones of Ethiopia are diverse and range from arid, semi-arid, humid to moist (Figure 2b).

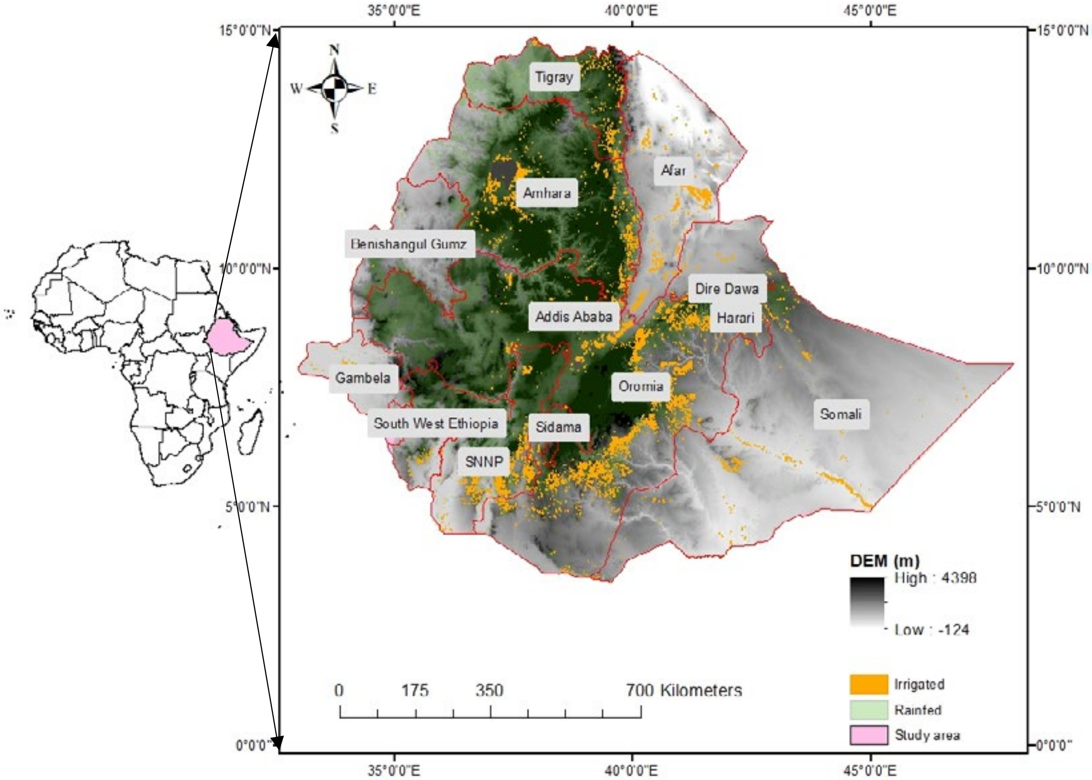

Figure 1: Rainfed and Irrigated Areas in Ethiopia:Food and Agriculture Organization (FAO)Water Productivity (WaPOR) and Hillshade of the Digital Elevation Model (DEM). The Red Borders Delineate the 13Administrative Regions of Ethiopia (SNNP Denotes Southern Nations, Nationalities, and Peoples).

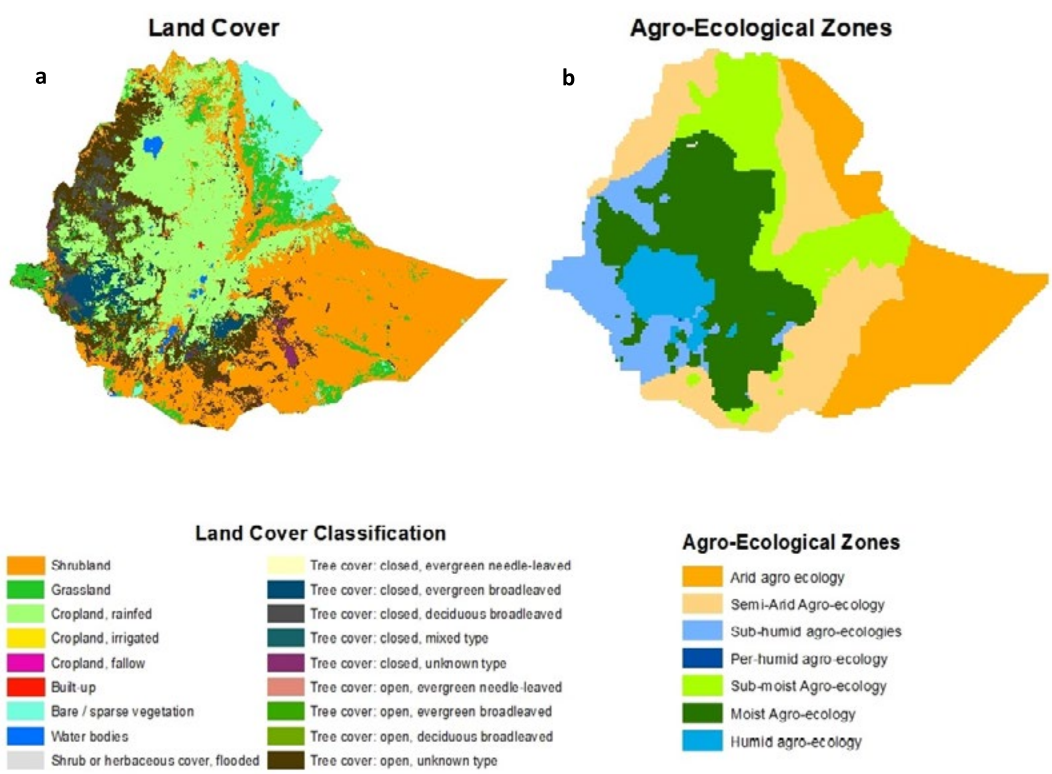

Figure 2: Land Cover Classification and Agro-Ecological Zones of Ethiopia. Source: Land Cover Classification from Food and Agriculture Organization (FAO) Water Productivity (WaPOR) 2022 and Agro-Ecological Zone Data from the International Food Policy Research (IFPRI) and FAO.

2.2 Crop Distribution in Ethiopia

Ethiopia has a diverse climate and landscapes leading to diverse crops and flora. The International Food Policy Research (IFPRI) has documented the most important 36 crops using the Spatial Production Allocation Model (SPAM) planted and harvested across the country [21,22]. Ethiopia has a diverse and complex landscape, climate, and agro-ecological conditions. This results in substantial variation in crops produced across the country (Figure 4). The five major cereals (*teff*, wheat, maize, sorghum, and barley) constitute the core of agriculture and food economy accounting for 77% of the total area cultivated and 29 percent of GDP [23,24].

Pulses, oilseeds, and fruits and vegetables account for 5%, 3%, 1.5% of the agricultural GDP, respectively. Cash crops such as coffee, cotton, and *khat* account for a significant portion of the agricultural and total GDP. Coffee, for example, accounts for 4–5% of GDP, 10% of total agriculture production, 40% of total exports, 10% of total government revenue, and 25–30% of total export earnings [25].

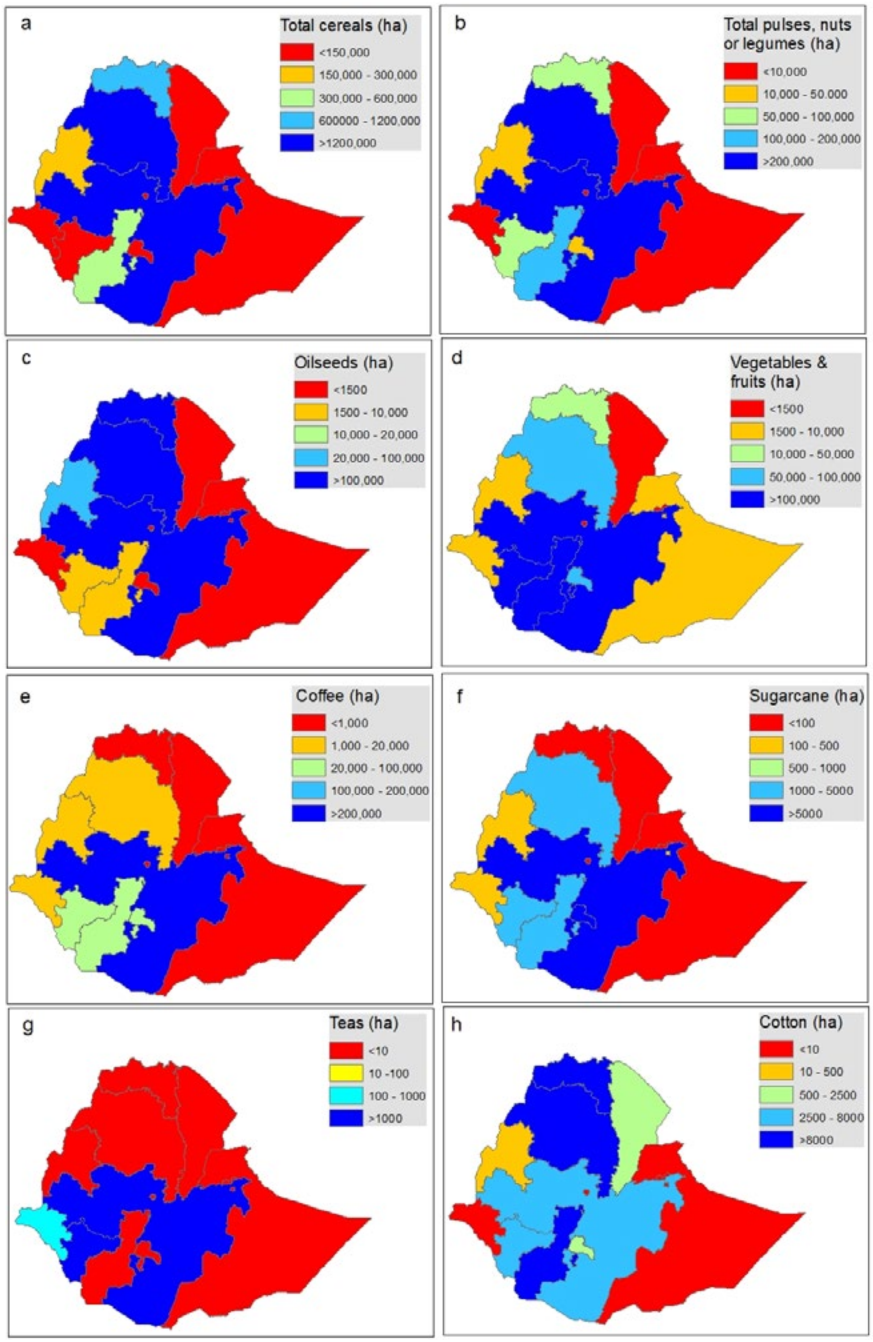

Figure 3: Estimated Distribution of Total Cereals (a) Pulses, Nuts, Legumes, and Oilseeds (b), Fruits and Vegetables, (c) Coffee, (d), Sugarcane, (e) Tea, (f) and Cotton, (g) Growing Areas Per Each Region of Ethiopia.

Source: International Food Policy Research Institute; Spatial Production Allocation Model (SPAM) Dataset

2.3 Available Data in Ethiopia

Several datasets were used to explore the impact of climate change on rainfed agriculture (Table 1). Datasets for current crop distribution of 36 crops across Ethiopia were obtained from IFPRI at 10 km resolution (Figure 3). Crop coefficient (*Kc*) values, root zone depths, and length of growing periods for each crop were gathered from the body of literature. Soil distribution data was obtained from International Soil Reference and Information Centre (ISRC) while irrigated and rainfed areas were obtained from International Water Management Institute (IWMI) and FAO monitor Water Productivity Open Access portal (WaPOR). WaPOR alsoprovidedgeneral land use land cover data for the country. Historical climate data were obtained from Ethiopian Meteorological Institute and Climate Hazards Group InfraRed Precipitation with Station (CHIRPS) and Modern-Era Retrospective Analysis for Research and Applications (MERRA) data. Downscaled CMIP5 climate projections data were obtained from IPCC. Each dataset is described in detail in its respective section within the methodology.

Data	Source	Resolution	Type
Crop coefficient (Kc)	Literature	Various	Various
Growing period	Literature	Various	Various
Root depth (zr)	Literature	Various	Various
Leaf area index (LAI)	Literature	Various	Various
Maximum root depth (zr,max)	Literature	Various	Various
Historical climate	EMI/CHIRPS/MERRA	station points/~4 km	Point/Raster
Projected climate	IPCC/Downscaled CMIP5	~ 25 km	Raster
Crop Planting/Harvesting dates	FAO	-	CSV
Agro-Ecological Zone (AEZ)	FAO	-	Vector
Rainfed area	IWMI/FAO WaPoR	100 m	Raster
Irrigated area	IWMI/FAO WaPoR	100 m	Raster
Land use land cover	FAO WaPOR	30m	Raster
36 Crop Types	IFPRI/SPAM	10km	Raster
Soil Distribution	ISRIC world soil information	-	Vector
Administrative Boundaries	Central Statistics Agency	-	Vector

Table 1: Summary of Data Sources, Literature, Resolution, and Type

2.4 Modeling Approach

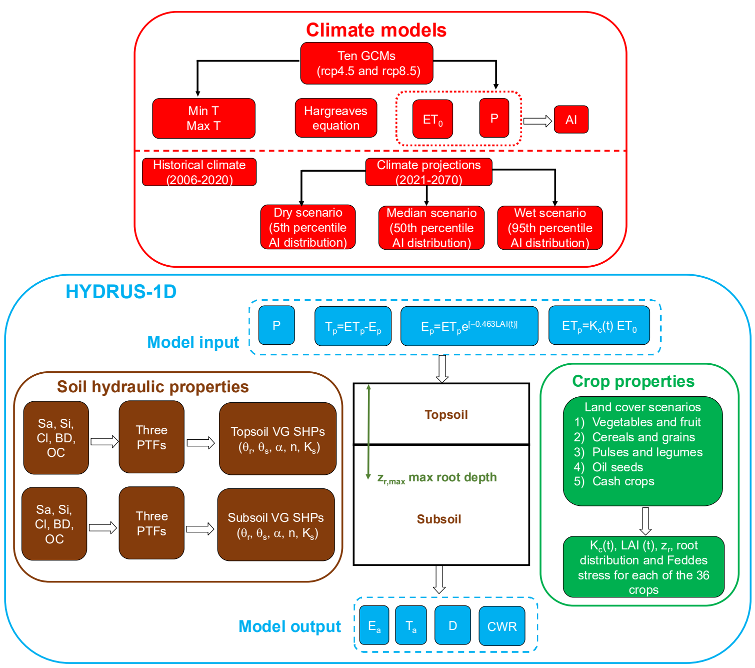

Figure 4: Schematic Overview of the Model Approach Used in this Study.

The IFPRI Crop Distribution Map in Ethiopia Comprises a Total of 6,495 Pixels in Which the Following Data and Information are Available: *i*) The Soil Physical Properties, Namely Sand (Sa, %), Silt (Si, %), Clay (Cl, %), Organic Carbon (Oc, %) and Soil Bulk Density (Bd, G Cm^{-3}) for Topsoil (0-30 Cm Soil Depth) and Subsoil (30-100 Cm Soil Depth) Used as Predictors in Three Pedotransfer Functions (Ptfs) to Estimate the Soil Hydraulic Properties (Vg Shps, Namely *Θr, Θs, Α, N* And K_s) Proposed by Van Genuchten

(1980) (Brown Box); *Ii*) The Minimum (Min T) and Maximum (Max T) Temperature and Precipitation/Rainfall (P) at Daily Time Resolution Were Taken from Ten General Circulation Models (GCMs) with Two Contrasting Representative Concentration Pathways (Rcps) (Red Box); *iii*) Crop Characteristics Compiled from Literature for the Main Five Land Cover Classes, Namely the Crop Coefficient (K_c), Leaf Area Index (LAI), Maximum Root Depth ($Z_{r,Max}$), Root Distribution, and Prescribed Soil Matric Potential Values Controlling Root Water Uptake Stress (Feddes Parameters) (Green Box). An Ensemble of Simulations in Hydrus-1d Were Run (Cyan Box) By Changing Daily P and Crop-Specific Potential Evapotranspiration (Et_p) In 2005-2050 Derived from Historical and Three Contrasting Projected (5^{th}, 50^{th}, 95^{th} Percentiles of Ai Distribution) Scenarios Based on the Fao Aridity Index (AI). In Each Model Simulation the Actual Evaporation (e_a), Actual Transpiration (t_a), Drainage (d) and Crop Water Requirement (CWR) Were Stored as Model Output. A Total of 935,280 (6495 Pixels × 36 Crops × 4 Modeling Scenarios) Numerical Simulations Were Carried Out in HYDRUS-1D.

Figure 4 displays the modeling approach used in this study. The FAO crop distribution map (10 km grid size) in Ethiopia comprises a total of 6,495 pixels. In each pixel data retrieved:*i*) the soil physical properties, namely sand (Sa, %), silt (Si, %), clay (Cl, %), organic carbon (OC, %), and soil bulk density (BD, g cm^{-3}) for topsoil (0-30 cm soil depth) and subsoil (30-100 cm soil depth) as predictors in three well-established Pedotransfer Functions (PTFs) to estimate the soil hydraulic properties (SHPs); *ii*) the minimum and maximum temperature and precipitation data at daily time resolution taken from ten General Circulation Models (GCMs) with two contrasting representative concentration pathway (RCPs); *iii*) crop characteristics taken from literature, namely the crop coefficient (K_c), leaf area index (LAI), maximum root depth (*zr*) and prescribed soil matric potential values controlling root water uptake stress (Feddes parameters) for each of the 36 crops.

An ensemble of numerical simulations in HYDRUS-1D was run (cyan box) in each pixel by changing daily precipitation (P) and crop-specific potential evapotranspiration (ET_p) from 2006 to 2070 (65 year-long time series) to get simulation output (E_a, T_a, D, and CWR). The output data were aggregated in annual sums.

The historical climate scenario (ranging between 2006 and 2020; 15-year-long time series) was compared with three projected climate scenarios (ranging between 2021 and 2070; 50-year-long time series) based on the aridity index (AI) frequency distribution: 1) dry climate scenario (5^{th} percentile of AI distribution); 2) median climate scenario (50^{th} percentile of AI distribution); 3) wet climate scenario (95^{th} percentile of AI distribution). Finally, a total of 935,280 (6,495 pixels × 36 crops × 4 modeling scenarios) numerical simulations were carried out in this study.

2.5 Climate Change Scenario Modeling

Ten General Circulation Models (GCMs) that have performed well in the country and are considered representative by the Ethiopian Meteorological Institute (EMI) and the Ministry of Water and Energy (MoWE) were selected for water supply projection to evaluate the impact of climate change on rainfed agriculture in Ethiopia[26]. Because the climate change scenarios were designed to help in future water resources planning and management purposes the moderate representative concentration pathway (RCP4.5) and the most pessimistic scenario (RCP8.5)were selected as climate change scenarios for the analysis.

The RCPs represent possible ranges of radiative forcing values in the year 2100 relative to pre-industrial values of +4.5 and +8.5 W/m^2, respectively). Emissions in RCP4.5 peak around 2040 and 2080 then decline while the RCP 8.5 scenarios assume emissions continue to rise throughout the 21^{st} Century. A total of 20 climate projections (2 emission scenarios over 10 climate models) were evaluated. The FAO AI was used to rank the twenty climate models and select the 5^{th}, 50^{th}, and 95^{th} percentiles to represent extremely dry, median (most probable), and extremely wet climate scenario conditions [27,28].

The aridity index is described as the annual mean P over the annual mean grass-reference evapotranspiration, ET_0 ($AI = P/ET_0$) and is commonly used for climate classification [29]. AI distinguishes between arid or semi-arid (ASA, 0.05 <AI□0.50), dry or sub-humid (DSH, 0.50 <AI□0.75), and humid (H, AI > 0.75) climate classes. Both historic and projected climate data contain daily values of precipitation, and minimum and maximum temperatures obtained from CHIRPS and IPCC. Due to lack of data for wind speed, relative humidity, and solar radiation, it was necessary to use the temperature-based Hargreaves equation rather than the data intensive Penman-Monteith formula to estimate reference crop evapotranspiration, ET0 [30,31].

The formula only requires minimum and maximum temperature data while the extraterrestrial radiation is estimated by using study site (pixel) latitude and day of the year [32]. The crop coefficient (*Kc*) converts ET_0 (index of climatic demand of reference grass) into specific-crop potential evapotranspiration (ET_p) under standard conditions and without water limitations. The leaf area index (LAI) is used to partition ET_p into potential evaporation (E_p) and potential transpiration (T_p) by using the following equation:

$$E_P = ET_p e^{-kLAI} \quad [1]$$

where κ (-) is the dimensionless extinction coefficient for global solar radiation inside the canopy and is assumed to be equal to 0.463 [33]. The *LAI* determines the amount of precipitation interception (*PI*) that is subtracted from P to obtain net precipitation (P_{net}) falling on the soil surface:

$$PI = aLAI\left(1 - \frac{1}{1 + b\frac{P}{aLAI}}\right) \quad [2]$$

where a (cm d-1) is an empirical coefficient, assumed as 0.025 cm d-1 and b (-) denotes the soil cover fraction given by:

$$b = 1-e^{-kLAI} \quad [3]$$

It is worth noting that considering Pnet instead of total precipitation accounts for precipitation that can be intercepted by foliage cover and does not reach the soil surface [34,35]. The main crop characteristics (K_c, LAI, and $z_{r,max}$) of the 36 crops in Ethiopia are listed in Table 2 according to different growth stages (initial, development and late growing stage).

		Kc			LAI			$z_{r,max}$
Crop	**Classification**	**IS**	**DS**	**LGS**	**IS**	**DS**	**LGS**	
					$m^2 m^{-2}$	$m^2 m^{-2}$	$m^2 m^{-2}$	m
Apple	Vegetable and fruit	0.60	0.95	0.65	0.00	2.46	2.46	1.10
Banana	Vegetable and fruit	0.50	1.10	1.00	0.62	2.57	2.57	0.90
Barley	Cereals/grains	0.30	1.13	0.33	0.10	0.80	0.80	1.50
Bean	Pulses, nuts, or legumes	0.40	1.15	0.90	0.50	2.00	2.00	0.70
Cabbage	Vegetable and fruit	0.45	1.00	0.95	0.10	4.00	4.00	0.80
Cassava	Vegetable and fruit	0.30	0.80	0.30	0.10	7.00	7.00	1.00
Chickpea	Pulses, nuts, or legumes	0.40	1.00	0.35	0.50	3.50	3.50	1.00
Cocoa	Vegetable and fruit	1.00	1.05	1.05	0.10	4.00	4.00	1.00
Coconut	Vegetable and fruit	0.54	0.73	0.65	0.10	2.40	2.40	1.00
Coffee	Cash crops	1.05	1.10	1.10	0.10	4.40	4.40	1.50
Cotton	Cash crops	0.35	1.17	0.60	0.11	5.57	5.57	1.70
Cowpea	Pulses, nuts, or legumes	0.40	1.00	0.35	0.50	3.50	3.50	1.00
Groundnut	Pulses, nuts, or legumes	0.40	1.15	0.60	0.10	5.90	5.90	1.00
Lentil	Pulses, nuts, or legumes	0.40	1.15	0.30	0.10	7.00	7.00	0.80
Maize	Cereals/grains	0.30	1.20	0.45	0.12	5.98	5.98	1.70
Millet	Cereals/grains	0.30	1.13	0.33	0.20	4.90	4.90	2.00
Palm oil	Oil seeds	0.30	0.87	0.80	0.10	5.00	5.00	1.00
Olive	Vegetable and fruit	0.65	0.70	0.70	0.20	5.80	5.80	1.70
Orange	Vegetable and fruit	0.80	0.80	0.80	0.10	8.60	8.60	1.70
Pigeonpea	Pulses, nuts, or legumes	0.40	1.00	0.35	0.50	3.50	3.50	1.00
Plantain	Vegetable and fruit	0.50	1.10	1.00	0.62	2.57	2.57	0.50
Potato	Vegetable and fruit	0.50	1.15	0.75	0.10	5.00	5.00	0.60
Rapeseed	Oil seeds	0.35	1.07	0.35	0.10	3.80	3.80	1.50
Rice	Cereals/grains	1.05	1.20	0.75	0.12	5.98	5.98	1.00
Sesameseed	Oil seeds	0.35	1.10	0.25	0.10	3.58	3.58	1.50
Sorghum	Cereals/grains	0.45	1.18	0.78	0.20	4.90	4.90	2.00
Soybean	Pulses, nuts, or legumes	0.40	1.15	0.30	0.10	5.51	5.51	1.30
Sugarbeet	Vegetable and fruit	0.35	1.20	0.70	0.10	3.00	3.00	1.20
Sugarcane	Cash crops	0.40	1.25	0.75	0.10	4.50	4.50	2.00
Sunflower	Oil seeds	0.35	1.07	0.25	0.10	4.20	4.20	1.50
Sweet potato	Vegetable and fruit	0.50	1.15	0.65	0.10	6.50	6.50	1.50
Tea	Cash crops	0.95	1.00	1.00	0.20	4.90	4.90	1.50
Teff	Cereals/grains	0.60	1.10	0.80	0.10	5.36	5.36	1.00
Tobacco	Cash crops	0.35	1.10	0.95	1.00	2.50	2.50	0.70
Wheat	Cereals/grains	0.30	1.15	0.32	0.10	6.00	6.00	1.80
Yams	Vegetable and fruit	0.50	1.15	0.65	0.10	6.37	6.37	0.40

Table 2: Crop Coefficient (kc), Leaf Area Index (lai) and Maximum Root Depth (zr,max) at Initial (is), Development (ds) and Late Growing Stage (lgs) Used for the 36 Crops in Ethiopia.

2.6 Numerical Modeling Using HYDRUS 1-D

The water balance in the soil-plant-atmosphere system was numerically evaluated using HYDRUS 1-D in each pixel by using the Richards equation:

$$\frac{\partial\theta}{\partial t} = \frac{1}{\partial z}\partial\left[K(\psi)\left(\frac{\partial\psi}{\partial z}+1\right)\right] - \xi(z,\psi,T_p) \quad [4]$$

where t (d) is time, z (cm) is soil depth (positive upward), ψ is the soil water pressure head (cm), θ ($cm^3\ cm^{-3}$) is the soil volumetric water content, and ξ (z, ψ, T_p) is the actual root water uptake sink term (d^{-1}) depending on soil depth, soil pressure head and potential transpiration (T_p). The soil water retention function $\theta(\psi)$ is described by van Genuchten's equation [36,37].

$$\theta(\psi) = \theta_r + \frac{\theta_s - \theta_r}{[1+(|\alpha|^n)]^m} \quad [5]$$

where α (cm^{-1}), m (-) and n (-) are water retention shape parameters, θ_r ($cm^3\ cm^{-3}$) and θ_s($cm^3\ cm^{-3}$) are residual and saturated water contents, respectively. The two parameters m and n are related with the condition $m = 1-1/n$[37,38].

Considering the degree of saturation, $Se = (\theta-\theta_r) / (\theta_s-\theta_r)$, which varies from 0 ($\theta = \theta_r$) to 1 ($\theta = \theta_s$), the unsaturated hydraulic conductivity function, K(Se) is given by the following equation:

$$K(S_e) = K_s S_e^{\tau}\left[1-\left(1-S_e^{1/m}\right)^m\right]^2 \quad [6]$$

where K_s (cm d^{-1}) is the saturated hydraulic conductivity and τ (-) represents the tortuosity parameter that is assumed to be $\tau = 0.5$ [38]. In data-poor countries such as Ethiopia, the direct measurement of several gridded soil hydraulic properties would be impractical and unfeasible, therefore the four unknown (θ_r, θ_s, α, n) soil hydraulic parameters of the van Genuchten's water retention function were estimated by using three well-established Pedotransfer Functions (PTFs) based on easily reproducible empirical regression relationships: *i*) WOS99 PTF; *ii*) ROSETTA PTF; *iii*) WEY09 PTF [39-43]. These three PTFs were used to predict the water retention in each pixel of the FAO soil distribution map providing sand, silt, clay, organic carbon, and soil bulk density.

The water content values corresponding to 30 prescribed pressure head values, ranging from near-saturation ($\psi = 10^0$ cm) to wilting point ($\psi = 10^{4.2}$) cm,were calculated from each of the three sets of parameters. A total of 90 water retention data pairs was obtained in each pixel. The four soil hydraulic parameters(α, n, θ_r, θ_s) were fit to obtainthe water retention function in each pixel.

The last unknown parameter, K_s, is even more difficult to estimate from easily available soil physical properties [44]. In this study K_s was estimated by using the Guarracino's formula based on θ_s and α[40,45]. This formula proved to be reliable as prediction uncertainty was bounded within three orders of magnitude in two international datasets [46].

The depth of the soil profile was assumed to be 200 cm and divided in topsoil (z = 0-30 cm) and subsoil (z = 30-200 cm). When the FAO map does not report subsoil soil physical-chemical properties, a homogenous soil profile with topsoil parameters was assumed. The lower boundary condition was set to free drainage to obtain downward water flux (D) across the soil profile bottom while P_{net} and E_p represent the system-dependent time-variable daily water fluxes of the upper boundary condition. T_p determines the potential root water uptake and depends on time-variant root depth (z_r).

Root distribution was assumed to be linear along the soil profile by varying from maximum at the soil surface to minimum at time-variant z_r. Both E_p and T_p are reduced by water limitation into actual evaporation (E_a) and actual transpiration (T_a).The stress response function is a piecewise linear reduction function proposed by, which depends on prescribed pressure head values [47]. HYDRUS 1-D includes a dataset of specific-crop root water stress parameters.Initial conditions were set in terms of pressure head values along the soil profile to set hydraulic equilibrium.

The input (P, E_p, T_p) and output (T_a,E^a, and D) fluxes simulated in Hydrus-1D were aggregated in annual sums for further data analysis.

2.7 Crop Water Requirement (CWR) Analysis

Crop water requirement (CWR) is usually referred to crop-specific potential evapotranspiration, however in this study we opt to define CWR as the difference between potential (T_p) and actual (T_a) transpiration:

$$CWR = T_p - T_a \quad [7]$$

In other words, CWR refers to the amount of water required to minimize drought stress. This amount of water depends on climate-dependent soil water storage dynamics and also on soil hydraulic properties (Eq. 5 and Eq. 6) and crop characteristics (K_c, LAI, $z_{r,max}$, Feddes parameters). The model setup in HYDRUS 1-D allows the use of time-variant vegetation parameters of the 36 crops, which was obtained from values in the scientific body of literature. As the crop develops, ground cover, crop height, LAI, and root depth change in time. Therefore, we distinguished between annuals and perennials for different crop growing stages (initial phase, crop development, and late season) and for the dormant season.

The total number of numerical simulations in HYDRUS-1D included: (a) numerical simulation under "historic" climate conditions (a total of 5,479 days between 2006 and 2020) for 36 crops; (b) three numerical simulation scenariosunder future climate projections (a total of 18,262 days between 2021 and 2070).

The crop water requirement (CWR) was calculated for each pixel and each crop by considering crop growing season and crop characteristics such as leaf area index and root depth. The relationship between mean annual CWR and AI was expressed with the following exponential regression equation:

$$CWR = a\, e^{bAI} \quad [8]$$

with *a* and *b* are regression parameters optimized on observed AI and simulated CWR data pairs and corresponding coefficient of determination (R^2) expressing the model fitting quality. The coefficient *a* is a proxy of the maximum CWR while the coefficient *b* controls the sensitivity between AI and CWR. In other words, CWR decays exponentially from arid to humid conditions for the same crop and more negative *b* implies a steeper decay in CWR wherelower CWR implies less root water uptake stress.

2.8 Sensitivity Analysis

The sensitivity analysis helpsanalyze the CWR changes in response to spatio-temporal changes in precipitation, and evapotranspiration. In this study, AI was considered the main systemic driving force related to changes in CWR. The relationship between change in AI (ΔAI) and in CWR (ΔCWR) was expressed with the following linear regression equation:

$$\Delta CWR = c\Delta AI + d \quad [9]$$

where *c* and *d* are regression parameters fitted on observed ΔAI and simulated ΔCWR data pairs. The corresponding coefficient of determination (R^2) expresses the model fitting quality.

3. Results and Discussion

3.1 Historical Climate Conditions

Ethiopia is markedly heterogeneous and geographical characteristics such as variable orography and continental-scale atmospheric processes (Indian and tropical configurations) induce highly variable temperature (T; Figure.5a) and rainfall (P; Figure. 5b) patterns.The spatial-average mean annual grass-reference potential evapotranspiration (ET0; Figure.5c) is 1,763.9 mm with a standard deviation (SD) of 166.7 mm and a coefficient of variation (CV) of about 10%. This low spatial variability is explained mostly by the mean annual temperature patterns,which varies over space depending on different elevations in mountainousEthiopia (Figure.5a).

According to the temperature-based Hargreaves formula, daily ET_0 is calculated usingdaily minimum, maximum and mean air temperature, and location latitude. The coldest temperatures (8.7-19.3°C corresponding to 1st - 25th percentiles) were recorded over mountainous regions in central, northern, and northeastern Ethiopia, while the warmest temperatures (23.6-31.0°C corresponding to 75th - 99th percentiles) were generally found in the lowlands of northeast and southeast.

The mean annual rainfall in Ethiopia ranged between 119.3 - 631.2 mm (1st - 25th percentiles) in the eastern lowlands to 1,089.5-2,419.0 mm (75th - 99th percentiles) in the southwestern region with a mean value of 1,074.8 mm under the historical conditions. Rainfall is influenced by tropical and extratropical circulations (ENSO) as well as the Indian monsoon system that brings substantial moisture from the Indian Ocean [48].

The mean annual FAO AI mostly reflects the spatial patterns of the mean annual rainfall in Ethiopia. The spatial-average mean annual AI is 0.609 indicating dry climate class in Ethiopia with humid zones in the central and western parts and arid regions in the eastern lowlands (Figure. 5d). Nearly 53% of the national territory is under arid conditions (AI<0.5) while the remaining portion of Ethiopia lies under mid (35%) and humid (12%) conditions (Figure. 5e).

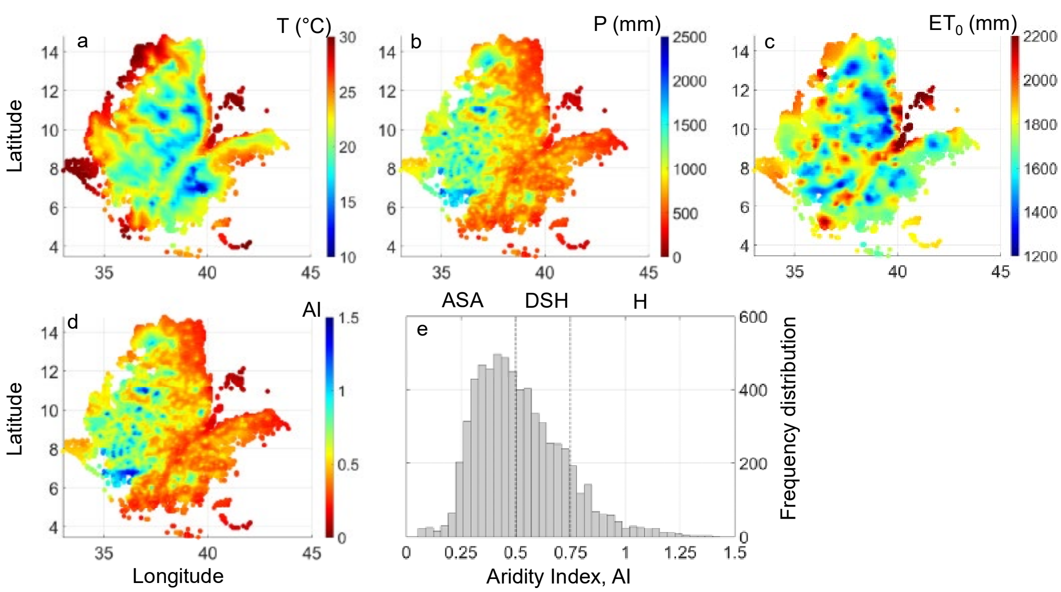

Figure 5: Spatial Distribution of Mean Annual a) Air Temperature, T (°C), b) Rainfall, P (mm), c) Grass-Reference Potential Evapotranspiration, Et_0 (Mm), D) Fao Aridity Index (Ai) And E) Frequency Distribution of Fao Aridity Index (Ai) Under Historical Climate Conditions (2006-2020) in Ethiopia. Vertical Dashed Lines Delimit Arid or Semi-Arid (ASA, 0.05 < AI ≤ 0.50), Dry or Sub-Humid (Dsh, 0.50 < Ai ≤ 0.75), and Humid (H, Ai > 0.75) Climate Classes [29].

3.2 Projected Climatic Conditions

The GCMs were ranked according to the FAO AI and the majority forecast generally a more humid climate in Ethiopia with rise of mean annual P and ET_0 (Table 3). Only the CSIRO_MK360 (both RCPs), CCSM4 (both RCPs) and GFDL_ESM2M (RCP8.5) rank below historical climate by forecasting drier-than-normal climatic conditions in Ethiopia.Generally, pronounced reductions in rainfall are predicted in the arid lowlands near Somalia.The results agree with existing studies that reported reduction in rainfall and increased frequency of droughts in the Ethiopian lowlands [49-51].The IPSL_CM5A_LRand IPSL_CM5A_MR under both RCP4.5 and RCP8.5 forecast much wetter conditionsby 32 to 47% increase compared to the historical rainfall. The wetter conditions are predicted to intensify in the highlands of Ethiopia.A general increase in rainfall was also reported by [52]. All the GCMs predicted higher temperatures than the historicalby a range of 0.31 °C (CSIRO_MK360 RCP4.5) to 2.06 °C (IPSL_CM5A_LR RCP8.5). This result is consistent with a World Bank report that forecasted temperature rise in Ethiopia will range between 0.7 and 2.9 °C.

RCP	GCM	P	T	ET_0	AI
		mm	°C	mm	
4.5	CSIRO_MK360	1000.5	21.00	1843.5	0.543
8.5	CSIRO_MK360	1089.0	22.16	1847.4	0.589
8.5	CCSM4	1101.3	21.83	1842.2	0.598
4.5	CCSM4	1109.4	21.36	1835.9	0.604
8.5	GFDL_ESM2M	1117.9	22.11	1837.2	0.608
**	**Historical**	**1074.8**	**20.69**	**1763.9**	**0.609**
4.5	GFDL_ESM2M	1121.2	21.39	1830.3	0.613
4.5	GFDL_CM3	1149.7	21.91	1862.7	0.617
8.5	GFDL_CM3	1148.1	22.21	1858.9	0.618
8.5	CNRM_CM5	1144.7	21.73	1809.4	0.633
4.5	CNRM_CM5	1182.7	21.42	1804.4	0.655
8.5	MPI_ESM_LR	1255.5	22.57	1874.6	0.670
4.5	MPI_ESM_MR	1251.4	22.13	1859.4	0.673
4.5	MPI_ESM_LR	1256.0	22.10	1854.7	0.677
8.5	MPI_ESM_MR	1269.0	22.38	1869.8	0.679
4.5	CanESM2	1284.4	21.72	1814.9	0.708
8.5	CanESM2	1384.5	22.39	1835.2	0.754
4.5	IPSL_CM5A_LR	1418.0	22.21	1807.6	0.784
4.5	IPSL_CM5A_MR	1430.2	22.17	1805.4	0.792
8.5	IPSL_CM5A_MR	1546.0	22.59	1811.8	0.853
8.5	IPSL_CM5A_LR	1584.9	22.75	1835.5	0.863
** Historical data inserted for comparison					

Table 3: General Circulation Models (GCMs) Ranked by Using the Fao Aridity Index (AI). Representative Concentration Pathways, RCP, Spatial-Average Mean Annual Rainfall, P (mm), Temperature, T (°C), Grass-Reference Potential Evapotranspiration, ET0 (mm), and Aridity Index, Ai, Are Reported for Each GCM. AI Distinguishes Between Arid or Semi-Arid (ASA, 0.05 < AI ≤ 0.50), Dry or Sub-Humid (DSH, 0.50 < AI ≤ 0.75), and Humid (H, AI > 0.75) Climate Classes [29].

Despite the increasing trend of spatial-average mean annual ET_0 induced by warming temperatures, the three climate projections provided wetter-than-normal conditions under the median and wet scenario and kepta climate class similar to the historical situation only under the dry climate scenario (Figure .6).The most probable climate projection (with median AI) indicatesthat the areas under arid conditions are likely to halve from 53% to about 25%, especially in the central-eastern part of the country.Meanwhile, the dry or sub-humid, and humid regions will cover 35% and 37% of the national area, respectively.

The wet climate scenario projections indicatethat the regions under arid, dry or sub-humid, and humid conditions will be 20%, 18% and 62% of the country, respectively, whilethe dry scenario indicates that the regions under arid, dry or sub-humid, and humid conditions will be 37%, 41% and 22% of the country, respectively. Assessing drought changes using an ensemble of five Global Climate Models (GCMs) in the Coupled Model Intercomparison Project (CMIP5) over East Africa,found that drought will generally decrease in the Ethiopian highlands [53].

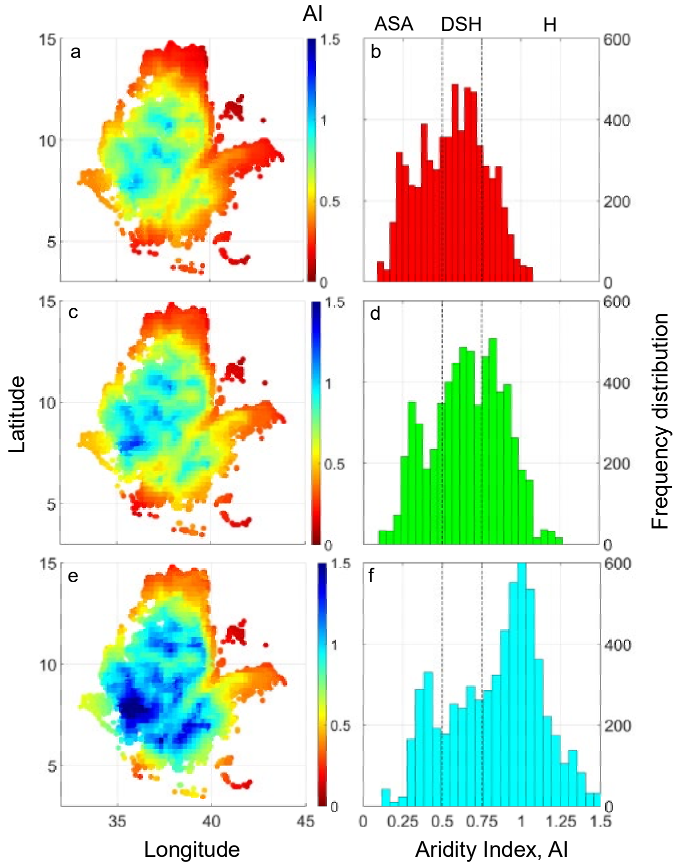

Figure 6: Spatial Distribution of Fao Ai Over the 6,495 Pixels in Ethiopia By Using A) Dry Climate Scenario (5th Percentile Gcm), C) Median Climate Scenario (50th Percentile Gcm), E) Wet Climate Scenario (95th Percentile Gcm), and Frequency Distribution of Fao Aridity Index (Ai) By Using B) Dry Climate Scenario (5th Percentile Gcm, Red Histograms), c) Median Climate Scenario (50th Percentile Gcm, Green Histograms), e) Wet Climate Scenario (95th Percentile Gcm, Cyan Histograms). Vertical Dashed Lines Delimit Arid or Semi-Arid (ASA, $0.05 < AI \leq 0.50$), Dry or Sub-Humid (DSH, $0.50 < AI \leq 0.75$), and Humid (H, $AI > 0.75$) Climate Classes [29].

Analysis of historical data from 1999 to 2014 shows that western regions are getting wetter and eastern regions are getting more arid [5]. Raised concern on the drying conditions in southern Ethiopia by analyzing gauged-based precipitation data during 1971-2011[54].However, several studies agree that rainfall is increasing in most parts of Ethiopia (except the eastern lowlands) induced by warming sea surface temperatures in the east Pacific and north Indian Ocean [55-57]. Further, the results also confirmed that changes in East Africa, including Ethiopia, follow the "dry gets drier and wet gets wetter" paradigm. The main advantage of selectingthree climate scenarios (dry, median, and wet climate scenarios) is thata range of climate conditions can be covered to account for variability while simultaneously reducing the number of model simulations [27,28].

3.3 The Relationship Between Crop Water Requirement and Aridity Index

The relationship between annual mean AI and CWR over the 6,495 pixels helpsprovide insight into any shift in climate conditions and related change in CWR. It is worth noting that the crop characteristics influencing root water stress are time-variant and change over different seasons (Table 2). Table 4 lists the CWR, the exponential regression(Equation. 8) coefficients (*a* and *b*)fitted on the data under historical and projected climate conditions for all crops.

The majority (34 out of 36) of crops are likely to experience a decrease in projected mean annual CWR induced by projected wetter climate. Only barley and plantain are likely to experience annual average increasesin root water stress induced by projected climate change. The increase in root water stress in barley compared to wheat could be related to thecrop characteristics (e.g.,LAI, K_c, and $z_{r,max}$) used in this study. For instance, if LAI and K_c are lower, the evapotranspirationdemand and partitioning will likely be more dominated by evaporation rather than transpiration. Under such circumstances, evaporation will not be sensitive to an increase in projected precipitation. However, the increase in projected stress in barley compared to wheat is likely related to the geographic coverage of barley crop plantation. Compared to barley, significantly more wheat is planted in the wet EthiopianHighlands that are projected to get wetter.As a result, wheat shows reduced crop water demand compared to the barley, which is planted in less abundance in the humid zones (Figure. 7).

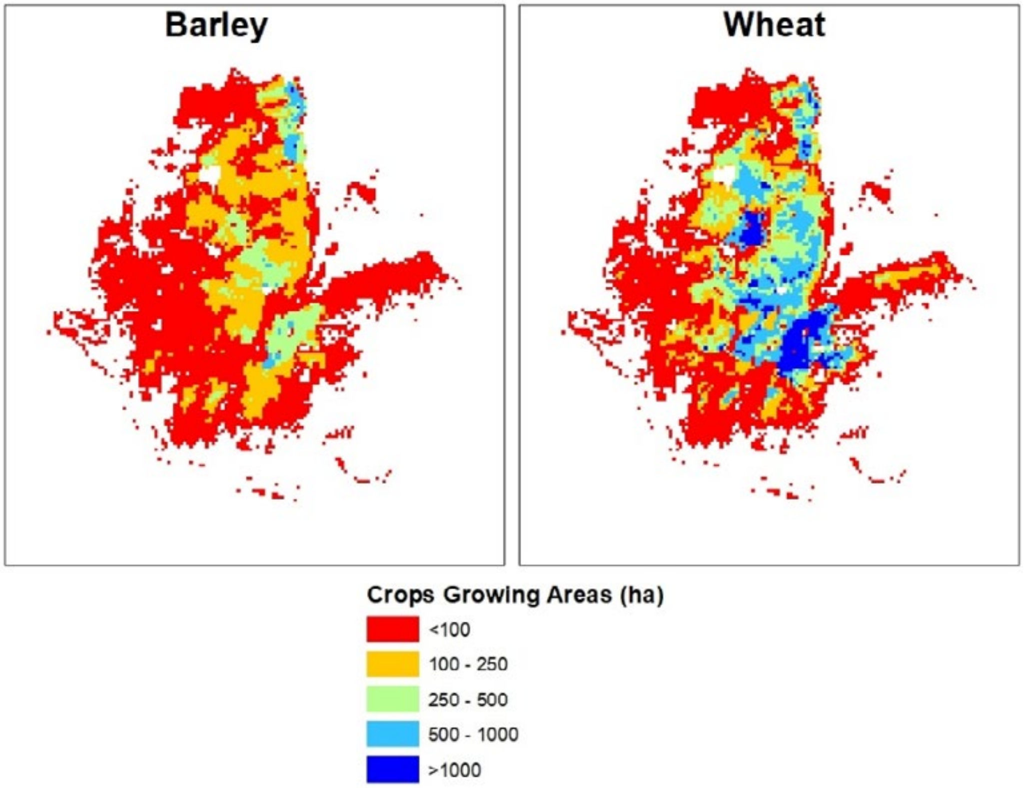

Figure 7: Coverages of Barley and Wheat Crop Planting Areas in Ethiopia.

FAO reports the crop water requirement for barley and wheat ranges between 450 mm to 600 mm for the total growing period and 1,200 mm to 2,200 mm for banana [58]. The CWR for plantain ranges between 900 mm to 1,700 mm in plantain, but its rainfed coverage in Ethiopia is insignificant [59]. Moderate decrease in CWR (less than 10%) is forecasted for apple, banana, cocoa, coconut, coffee, palm oil, tea, and tobacco.

The regression coefficients fitted on AI-CWR data highlight two aspects: *i*) coefficient *a* determines a scaling effect on the CWR and the comparison between historical and projected *a* coefficients indicates an upward or downward shift on the y-axis if projected *a* is higher or lower than historical *a*, respectively; *ii*) coefficient *b* dictates the shape of the decay function and the comparison between historical and projected *b* coefficients indicates a steeper or smoother decay if projected *b* is lower or higher than historical *a*, respectively; if *b* gets to 0, it signifies no sensitivity of CWR to AI.The analysis of *a* and *b* coefficients for the 36 crops revealed interesting dynamics.

The projected *a* coefficient of banana, bean, cassava, coconut, cowpea, millet, orange, sesameseed, sugarbeet, sugarcane, and sunflower, were lower than the corresponding historical values. This is expected because it reflected the corresponding decrease in mean annual CWR (Table 4). The projected *a* coefficient of the remaining crops contrasted the corresponding decreases in mean annual CWR. This result implies that,although a general wetting of the projected climate and a general decrease in CWR is observed, the projected root stress is likely to increase significantly over the arid regions of Ethiopia.

Further, this indicates that the most arid zones in the northern and eastern parts of the country are likely to experience dry shocks and droughtsunder the extremely dry conditionscenario. By contrast, the analysis of coefficient *b* reveals other dynamics. Apple, cabbage, groundnut, lentil, potato, rice, sweet potato, teff, and yams indicate the projected *b* coefficient that islower than the historical value. This result indicates that such crops will likely bemore sensitive to climate change in arid regions and less sensitive in humid regions of Ethiopia.

The remaining crops get the projected *b* value greater than the historical value where sensitivityof CRW to AI is reversed (i.e., crops are less sensitiveto climate change in the arid regions and highersensitivity in the humid regions). Therefore, the *b* coefficient might be informative to discriminate crops that are more sensitive in arid zones or those that are more sensitive in humid regions of Ethiopia.

The fitting quality was quantified through the coefficient of determination (R^2) and ranges between 0.02 (cowpea) and 0.93 (orange) in the baseline scenario and between 0.29 (potato) and 0.91 (orange) in the projected scenario. The fitting was generally good, especially for perennial crops and trees, with some few exceptions where R^2 values were very low, indicating poor relationship between AI and CWR (e.g., cowpea, groundnut, and potato) in the historical scenario.

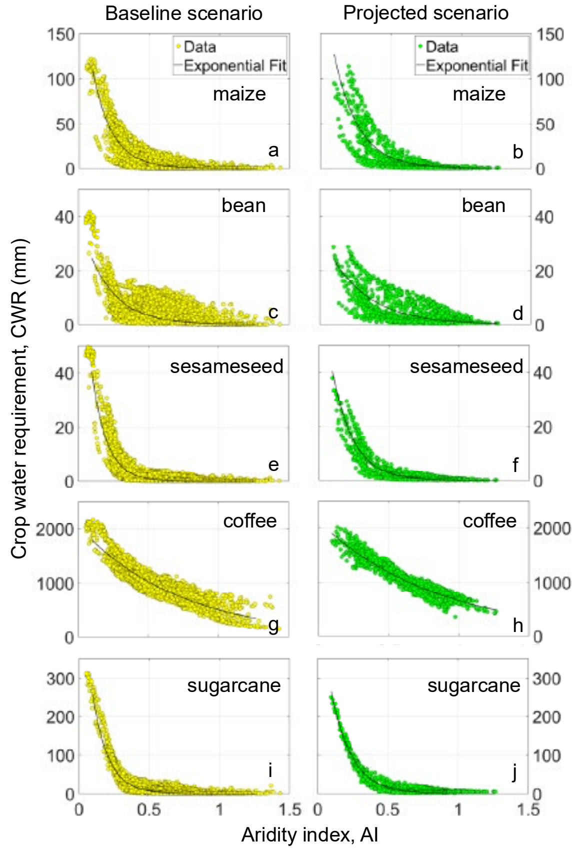

Figure 8: Relationship Between Mean Annual Fao Aridity Index and Crop Water Requirement (cwr) Under the Baseline (Historical) Scenario (Yellow Circles) For A) Maize, c) Bean, E) Sesameseed, G) Coffee, and I) Sugarcane, and Under Projected Scenario (Green Circles) For B) Maize, d) Bean, F) Sesameseed, H) Coffee, and J) Sugarcane. The Black Solid Line Indicates the Exponential Equation (eq. 8) Fitted on the Data.

Figure. 8 displays the exponential decay of CWR with respect to AI for maize, bean, sesameseed, coffee, and sugarcane representing important crop classesfor the cereals/grains, pulses/nuts/legumes, oilseeds, export commodity, and cash crops, respectively, under historical (Figure. 8, left panel, yellow circles) and projected (Figure. 8, right panel, green circles) climate conditions. The shift toward more humid climate conditions in the next decades reflects a decrease in crop root water stress and a different sensitivity between historical and projected conditions. Precipitation under climate change conditions has a positive and significant effect on water availability ofshort and long-term cereal crops production in Ethiopia [60].Coffee for instance is water-demanding (coffee has the highest CWR) and the climate shift toward more humid conditions is likely to induce a decrease in water stress and a weaker sensitivity of projected CWR to AI (Figure. 8g) when compared to the historical relationship (Figure. 8h).also reported that climate variables are the determining factorsfor coffee growing area suitability and that the combined (climate, topography, and soil characteristics) modeling variables predict suitability will increase [61].In contrast, also reported high correlation between climate change and coffee production but forecasted decrease in coffee production in Ethiopia [62]. It is also important to note that, except coffee, the crop water requirement of the crops (e.g., sugarcane) exponentially increases as aridity increases from sub-humid to semi-arid and arid conditions.

	Historical (2006-2020)				**Median scenario projection (2021-2070)**			
Crop	**Spatial-average CWR**	**a**	**b**	**R2**	**Spatial-average CWR**	**a**	**b**	**R2**
	mm				mm			
Apple	368.25	537.72	-0.75	0.38	345.85	588.60	-0.84	0.40
Banana	323.65	932.31	-2.16	0.88	301.88	903.49	-1.71	0.86
Barley	0.38	175.55	-13.17	0.83	0.48	102.93	-8.75	0.75
Bean	4.04	39.85	-4.95	0.41	2.76	34.80	-3.61	0.52
Cabbage	7.46	30.06	-2.31	0.14	4.34	70.48	-3.69	0.44
Cassava	8.16	309.20	-7.48	0.59	3.62	285.75	-5.83	0.68

Chickpea	11.75	68.61	-3.58	0.35	8.53	78.30	-3.18	0.50
Cocoa	937.67	1845.65	-1.36	0.83	911.30	1879.06	-1.10	0.84
Coconut	378.98	986.82	-1.90	0.80	354.35	978.66	-1.53	0.80
Coffee	1027.51	2057.77	-1.40	0.85	970.02	2105.71	-1.16	0.86
Cotton	17.00	459.31	-6.13	0.74	6.53	502.36	-5.55	0.76
Cowpea	7.12	73.82	-4.99	0.02	4.98	69.47	-3.82	0.57
Groundnut	16.50	84.81	-3.11	0.05	8.09	135.29	-3.79	0.52
Lentil	79.32	211.55	-1.95	0.24	52.12	335.72	-2.77	0.46
Maize	4.15	216.72	-7.12	0.80	1.78	223.45	-5.80	0.72
Millet	0.93	133.72	-8.84	0.78	0.66	116.84	-6.78	0.91
Palm oil	752.19	1590.89	-1.49	0.82	718.99	1608.34	-1.22	0.82
Olive	66.28	911.93	-5.15	0.82	29.32	979.34	-4.89	0.86
Orange	129.74	993.75	-4.20	0.93	60.98	950.79	-4.16	0.91
Pigeonpea	11.75	68.63	-3.58	0.35	8.53	78.30	-3.18	0.50
Plantain	3.53	272.34	-10.43	0.75	5.70	159.62	-5.80	0.79
Potato	30.95	58.54	-1.20	0.03	24.02	74.01	-1.61	0.29
Rapeseed	17.76	178.10	-4.92	0.40	9.81	202.39	-4.30	0.60
Rice	139.44	209.37	-0.83	0.18	110.99	260.16	-1.27	0.30
Sesameseed	1.14	101.79	-9.45	0.81	0.79	77.50	-6.65	0.86
Sorghum	19.67	276.18	-5.51	0.70	10.25	289.81	-4.71	0.77
Soybean	24.40	126.54	-3.36	0.46	17.39	141.92	-3.13	0.58
Sugarbeet	1.79	140.12	-8.69	0.75	1.03	124.58	-5.97	0.65
Sugarcane	9.63	604.93	-8.85	0.90	8.37	519.31	-6.89	0.91
Sunflower	1.38	107.91	-9.20	0.80	0.92	83.25	-6.43	0.85
Sweet potato	78.09	302.75	-2.79	0.42	46.69	428.14	-3.31	0.57
Tea	911.65	1921.83	-1.50	0.86	856.56	1949.97	-1.24	0.86
Teff	36.16	87.38	-1.73	0.33	28.63	108.27	-1.98	0.41
Tobacco	808.11	1569.54	-1.33	0.80	790.33	1589.83	-1.06	0.83
Wheat	22.48	375.31	-5.74	0.67	9.35	416.62	-5.03	0.70
Yams	126.90	236.37	-1.28	0.19	108.13	329.79	-1.76	0.39

Table 4: Spatial-Average Mean Annual Crop Water Requirement (Cwr), Regression Coefficients (A And B) Fitted on Ai and Cwr Data for the 36 Crops in Ethiopia Under the Historical (2006-2020) and the Most Probable Projected (2021-2070) Climate Conditions and Corresponding Coefficient of Determination (R2).

3.4 Sensitivity Analysis

The relationship between change in AI (ΔAI)and change in CWR (ΔCWR) describes the sensitivity of root water stress to climate characteristics in Ethiopia. In the linear regression model, the coefficient *c* denotes the slope of the regression line and *d* represents the intercept (Equation. 9). The steeper the slope, the more sensitive the change in CWR to the change in AI. Generally, the *c* coefficients are negative for all crops (Table 5) meaning thatan increasein climatic humidityis accompanied with a decrease in root stress. In other words, the more positive the change in AI, the more negative the change in CWR. Palm oil, apple, cocoa, coffee, plantain, rice, tea, and tobacco obtained the highest (less negative) *c* coefficientindicating relatively low sensitivity to climate change. The high R^2-values ($R^2 > 0.70$) indicate that annual level analysis may be enough to explain the relationship between CWR and AI in crops such as banana, cocoa, coconut, coffee, palm oil, tea, and tobacco. Most of the non-perennial crops, however, indicate low relationship ($R^2 < 0.50$) between CWR and AI. The crops with low R^2-values require detailed examination into the impact of seasonality of climate change with higher temporal resolution analytics.

Crop	c	d	R2
Apple	-0.408	9.23	0.50
Banana	-0.632	20.23	0.68
Barley	-0.623	18.43	0.20
Bean	-0.856	12.59	0.43
Cabbage	-0.847	8.09	0.46
Cassava	-0.855	2.62	0.40
Chickpea	-0.872	15.76	0.47
Cocoa	-0.502	19.16	0.72
Coconut	-0.654	22.67	0.73
Coffee	-0.520	18.74	0.73
Cotton	-0.896	1.19	0.43
Cowpea	-0.892	14.54	0.44
Groundnut	-0.905	6.08	0.52
Lentil	-0.795	6.86	0.54
Maize	-0.795	-7.83	0.34
Millet	-0.731	-7.97	0.28
Palm oil	-0.542	19.02	0.74
Olives	-0.952	6.54	0.53
Orange	-0.903	-0.92	0.62
Pigeonpea	-0.872	15.76	0.47
Plantain	-0.562	37.20	0.22
Potato	-0.677	10.26	0.42
Rapeseed	-0.934	11.41	0.51
Rice	-0.578	6.80	0.51
Sesameseed	-0.808	4.34	0.34
Sorghum	-0.948	9.32	0.49
Soybean	-0.889	15.03	0.50
Sugarbeet	-0.788	3.78	0.30
Sugarcane	-0.905	29.21	0.43
Sunflower	-0.808	2.32	0.34
Sweet potato	-0.907	9.42	0.59
Tea	-0.548	18.91	0.74
Teff	-0.761	14.68	0.48
Tobacco	-0.492	19.33	0.72
Wheat	-0.990	8.39	0.48
Yams	-0.649	13.09	0.48

Table 5: Regression Coefficients (*C* And *D*) Fitted on Change in Ai (ΔAi) and in Cwr (Δcwr) Data for the 36 Crops in Ethiopia and Corresponding Coefficient of Determination (R^2).

Figure. 9 illustrates the linear relationship occurring between the change in AI (ΔAI) and CWR (ΔCWR) for maize, bean, sesameseed, coffee, and sugarcane representing cereals/grains, pulses/nuts/legumes, oil seeds, export commodity, and cash crops, respectively. The figure shows that only coffee is characterized by low scatter ($R^2 = 0.73$) indicating that climate change impact on water stress in Ethiopia can be clearly observed. Meanwhile maize, bean, sesameseed, and sugarcane are affected by large data scattering depicting R^2-values of 0.34, 0.43, 0.34, and 0.30, respectively. This result indicates deep-dive studies into the seasonal dynamics of climate variability and the impact of related water stress onthese crops is critical to understand their vulnerability to climate change.

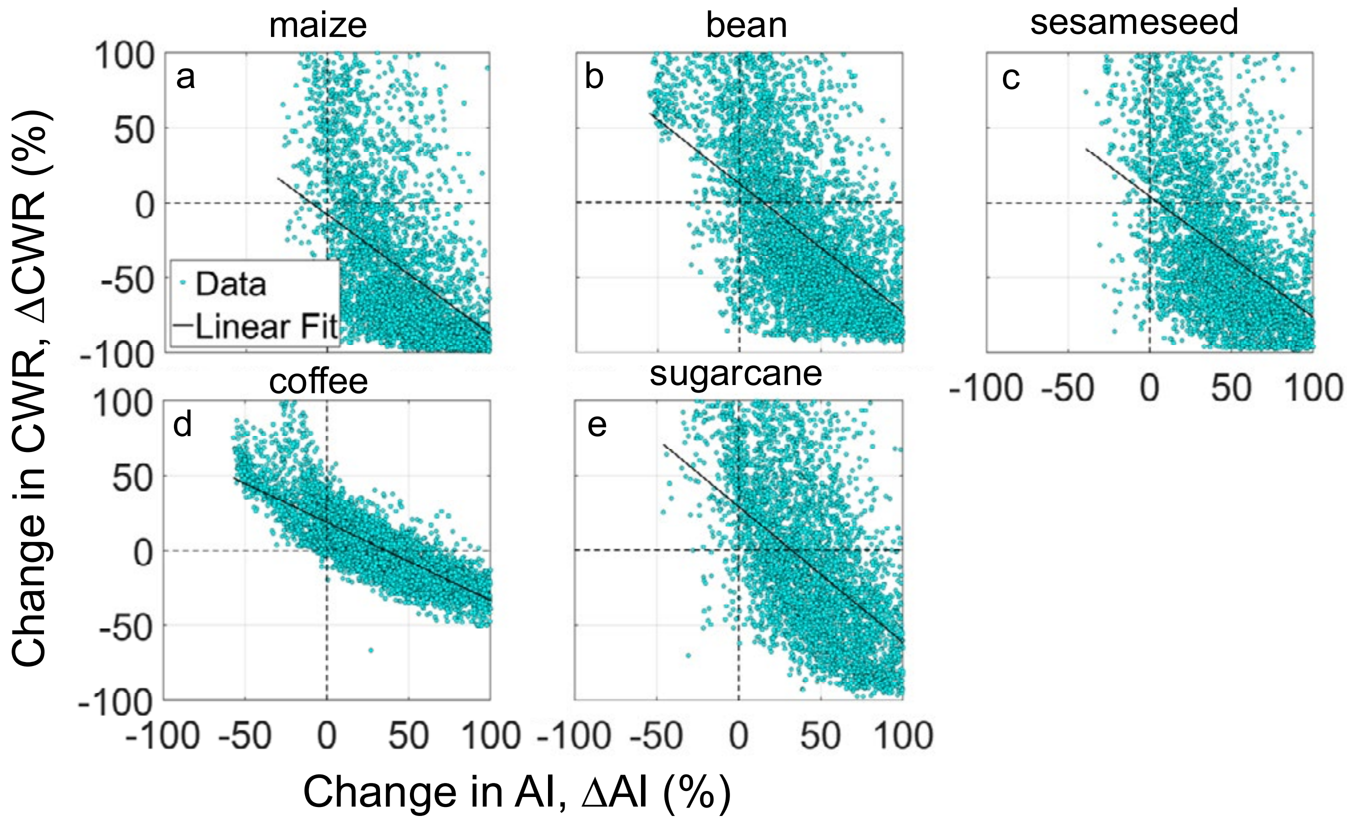

Figure 9: Relationship Between Change in Fao Aridity Index (ΔAi) and Crop Water Requirement (ΔCWR) for a) Maize, B) Bean, C) Sesameseed, D) Coffee, E) Sugarcane.

The spatial distribution of simulated CWR for each crop depended on soil properties, crop characteristics, and local climate conditions. Figure. 10 displays the distribution of CWR of the selected five important crops in each crop classification (maize, bean, sesameseed, coffee, and sugarcane) in Ethiopia under historical climate conditions (left panel).

The colors in the figure vary from reddish to bluish indicating high or low CWR in the left panel, respectively. In general, the highest CWR values are detected over the arid regions in Ethiopia. The lowest spatial-averageCWR belongs to sesamseed which appears less sensitive to droughtcompared to the other crops in this group. The fact that sesameseed has better capacity to withstand droughts and arid conditions more than other crops have also been reported by [63]. The panels on the right report the difference between projected (dry, median, wet scenarios) and historical CWR for each of the five analyzed crops. The difference in historical and projected CWR of maize, bean, sesameseed, and sugarcane vary over the same order of magnitudes (-20 to 20 mm) while CWR for coffee is much higher (-500 to 500 mm).

The regions that change color to yelloware those most sensitive to the projected climate. Northern Ethiopia appearsmore sensitive to climate change for maize, coffee, and sugarcaneand less sensitive for bean and sesamseed. By contrast, maize, coffee, and sugarcane in the central highlands of Ethiopia seem to reduce drought stressunder projected climate conditions, while bean and sesamseed keep CWR dynamics under both historical and projected climate conditions.

The impact of climate change on coffee is particularly observed in Southeastern Ethiopia where most of the Ethiopian coffee is produced. This region also hosts the Kaffa Biosphere Reserve known for its significant biodiversity and as theorigin of arabica coffee.

The best region for coffee in southwestern Ethiopia under historical climate conditions (bluish color in Figure. 10, fourth subplot in the left panel) is likely to undergo drier-than-normal climate by inducing increase in drought stress.This critical hotspot merits in-depth analysis to get a better understanding of potential impact of drought on water availability and crop production.

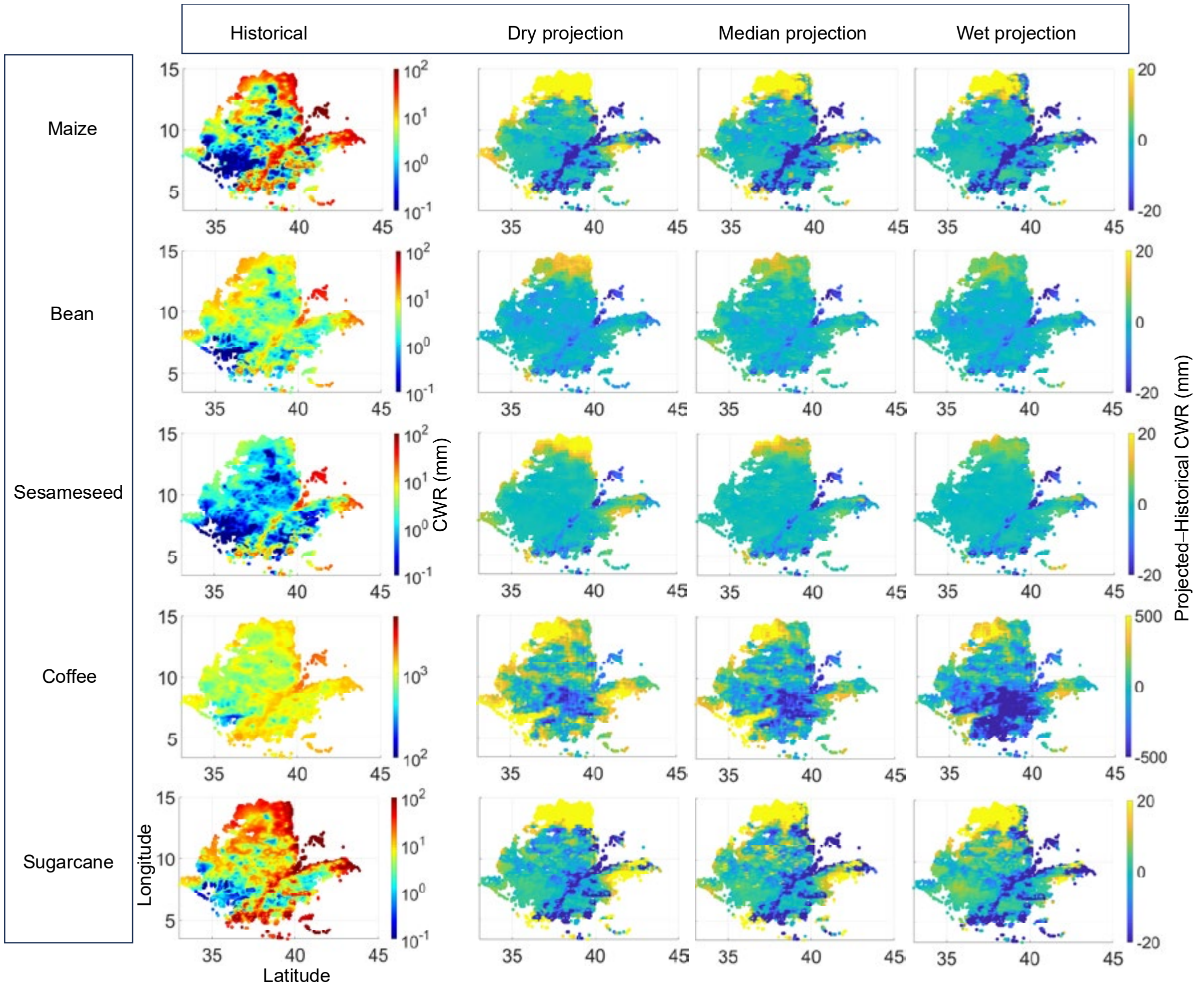

Figure 10: Crop Water Requirement (Cwr) for Maize, Bean, Sesameseed, Coffee, and Sugarcane Under Historical Climate Conditions (Colorbar from Blue to Red) and Difference Between Projected and Historical Cwr Under Dry, Median, and Wet Climate Scenarios (Colorbar From Blue to Yellow).

4. Limitations

This study is intended as a preliminary analysis to explore potentially critical hotspots and identify vulnerable crops to a changing climate in Ethiopia. As such,there are several limitations that should be considered when evaluating the results and derived conclusions and recommendations. These limitations include crop properties obtained from the literature, relatively coarse resolution for crop distribution, and soil properties obtained from Pedotransfer Functions.For example, the PTFs applied in this study are developed and calibrated in Europe and North America. Tropical PTFs are scarce and with even fewer validated datasets limiting the capacity to predict crop water requirements. The availability of global-scale digital maps of soil physical and chemical properties provides information at high-spatial-resolution to support the implementation of PTFs for modeling applications, such as Soil Grids 250mand its recently updated version, Soil Grids 2.0 [64-66]. However, such dataset in a large country like Ethiopia may have computational efforts with limited quality control.

Further, the soil physical and chemical properties obtained may not reflect the real heterogeneous spatial variability and as a result crop water demands may be dominated by climate patterns. The role of soil structure is alsoignored, and preferential flow was not modeled. This is a serious limitation in Ethiopia where crop tilling and similar crop field management are frequently practiced. Missing information on farm management, crop yield, and soil conservation practices was not included but can potentially be incorporated by coupling Hydrus-1D with DSSAT [67].

HYDRUS-1D is a well-known process-oriented, physically-based hydrological model applied in a myriad of studies. The application of a one-dimensional model over a heterogenous landscape (in terms of orography) by ignoring the effect of terrain attributes on surface and sub-lateral flow might compromise the model simulations. This aspect may be significant in the Ethiopian Highlandsand other areas where steep slope farming is practiced.

Concentrating on lowresolution temporal dynamics (i.e., annual averages) may also overlook the impact of seasonal variation in rainfall induced by climate change. High spatial and temporal resolution analytics in critical hotspots (e.g., arid and semi-arid) and vulnerable crops (e.g., coffee and maize)will follow this preliminary analysis.In addition, this approach will beenhanced in the future through more direct observations and including on-the-ground information on farming management practices.

5. Conclusion and Recommendations

Given the drastic impact of climate change on water resources, it is critical to understand the historical and projected crop water requirement in vulnerable countries such as Ethiopia. This exercise can help identify susceptible crops and vulnerable zones to water scarcity. Detailedanalysis on specific crops and seasonal dynamics can then focus on areas with high risk to climate impact.

In this study, the aridity index derived from potential evapotranspiration and precipitation was evaluated under historical and projected (dry, most probable, and wet) climate conditions. There is unanimous consensus among the 20 climate models that temperatures will riseranging from 0.3 to approximately 2 ^{o}C by the 21st Century. Almost all the climate models predict that rainfall is likely to increase in the central highlands of Ethiopia leading to a more humid climate condition. Because the changes in average annual temperatures are relatively low, the transformation toward increased or decreased aridity mainly depended on spatial changes in rainfall. While the most probable climate projection indicates that humid area coverage will likely increase from 25% to 37%, increases in temperature and pronounced reduction in rainfall around the northern, southern, and eastern borders will likely intensify aridity in the dryparts of Ethiopia. Further, pronounced reductions in rainfall are predicted in the arid lowlands near Somalia requiring further attention due to its historical vulnerability to dry shocks and potential intensification of droughts in the forecast.

Theimpact of climate change on the crop water requirement of the 36 major crops in Ethiopia was evaluated by comparing the crop water requirementunder the same historical and projected (dry, median, and wet) climate conditions. An ensemble of thousands numerical simulations in HYDRUS-1D was carried out by ensuring spatial distribution of soil hydraulic properties in a 2-m-thick layered soil profile (topsoil and subsoil) and spatio-temporal dynamics of crop characteristics (time-variant crop coefficient, leaf area index, maximum root depth, and crop-specific Feddes parameters) of each of the 36 crops.

The results indicate that, except for barley and plantain, most crops are likely to experience a decrease in projected mean annual crop water stressattributed to projected wetter climate. Because barley iscritical to food security in Ethiopia, deeper analytics may need to be carried out to fully understand vulnerability to food insecurity, livelihoods, and the national economy.

The relationship between crop water requirement and aridity index appears to be informative in discriminating between crops that are more sensitive to climate change in arid regions (e.g., *teff*, lentils, and potatoes) to those that are more sensitive in humid regions of Ethiopia. Teff, for instance, is the main staple food in Ethiopia grown by 6 million farmers and consumed by more than 50 million people and is critical for food security and livelihoods. As such, deeper analysis is imperative to understand its vulnerability to climate change in all regions. Similarly, the change in crop water requirement between historical and projected climate conditions for coffee was significant ranging -500 mm to 500 mm, indicating high vulnerability compared to other crops that ranged between -20 m and 20 mm. Because of the significance of coffee for the Ethiopian economy, deeper analyses with observation data and robust modeling are warranted.

The relationship between annual average crop water requirement and aridity index inmost of the non-perennial crops was not robust ($R^2 < 0.50$).The low relationship indicates that annually averaged values are not good predictors of susceptibility to climate change. The crops where low R^2-values were observed require detailed examination into the impact of seasonality of climate change with higher temporal resolution analytics.

While this study provides valuable insights into the impact of climate change on crops in Ethiopia, it should be noted that the analysis is subject to several limitations related to data and modeling approaches. Coarse spatial and temporal analytical resolutions,heavy reliance on global datasets, lack of farming practices information, and the 1-dimensional nature of the analytical model are limitations that require due considerations. Detailed analyses that address some of the described limitations will follow to further select few crops and critical hotspots that are most vulnerable to climate change and pose greater risk to food insecurity and the overall Ethiopian national economy.

Declaration of Competing Interest

The authors declare that they have no known competing financial interests or personal relationships that could have appeared to influence the work reported in this paper.

Data Availability

Data will be made available on request.

Acknowledgement

The authors would like to thank the Federal Ministry of Economic Cooperation and Development of Germany (BMZ) for their generous financial support under the Phase II BMZ-no: 2017. 9833.9 grant. We would also like to thank Eliza Swedenborg for her support in obtaining the grant and concept development.

References

1. *Agriculture and Food Security | Ethiopia | Basic Page | U.S. Agency for International Development*. (n.d.). Retrieved December 28, 2022, from https://www.usaid.gov/ethiopia/agriculture-and-food-security
2. *Ethiopia—Employment In Agriculture (% Of Total Employment)—2022 Data 2023 Forecast 1991-2020 Historica*l. (n.d.). Retrieved December 27, 2022, from https://tradingeconomics.com/ethiopia/employment-in-agriculture-

percent-of-total-employment-wb-data.html
3. Headey, D., Dereje, M., & Taffesse, A. S. (2014). Land constraints and agricultural intensification in Ethiopia: A village-level analysis of high-potential areas. *Food Policy, 48*, 129-141.
4. World Bank. A Country Study on the Economic Impacts of Climate Change, Environment and Natural Resource Management, Sustainable Development Department, Africa Region, Development Prospects Group. 2008 Report No. 46946-ET.
5. Brown, M. E., Funk, C., Pedreros, D., Korecha, D., Lemma, M., Rowland, J., ... & Verdin, J. (2017). A climate trend analysis of Ethiopia: examining subseasonal climate impacts on crops and pasture conditions. *Climatic Change, 142*, 169-182.
6. Weldearegay, S. K., & Tedla, D. G. (2018). Impact of climate variability on household food availability in Tigray, Ethiopia. *Agriculture & Food Security, 7*, 1-9.
7. Devereux, S., & Sussex, I. (2000). *Food insecurity in Ethiopia* (p. 7). Brighton, UK: Institute for Development Studies.
8. Gebreselassie, S., Kirui, O. K., & Mirzabaev, A. (2016). Economics of land degradation and improvement in Ethiopia. *Economics of land degradation and improvement–a global assessment for sustainable development*, 401-430.
9. Spielman, D. J., Kelemwork, D., & Alemu, D. (2011). Seed, fertilizer, and agricultural extension in Ethiopia. *Food and agriculture in Ethiopia: Progress and policy challenges, 74*, 84.
10. Van Loon, M. P., Deng, N., Grassini, P., Edreira, J. I. R., Wolde-Meskel, E., Baijukya, F., ... & van Ittersum, M. K. (2018). Prospect for increasing grain legume crop production in East Africa. *European Journal of Agronomy, 101*, 140-148.
11. *World Bank Climate Change Knowledge Portal*. (n.d.). Retrieved December 27, 2022, from https://climateknowledgeportal.worldbank.org/
12. *Climate change and its implications for rainfed agriculture in Ethiopia | Journal of Water and Climate Change | IWA Publishing*. (n.d.). Retrieved December 27, 2022, from https://iwaponline.com/jwcc/article/12/4/1229/75872/Climate-change-and-its-implications-for-rainfed
13. Simane, B., Beyene, H., Deressa, W., Kumie, A., Berhane, K., & Samet, J. (2016). Review of climate change and health in Ethiopia: status and gap analysis. E*thiopian Journal of Health Development, 30*(1), 28-41.
14. *Cereal yield (kg per hectare) | Data*. (n.d.). Retrieved December 28, 2022, from https://data.worldbank.org/indicator/AG.YLD.CREL.KG
15. Ketema, A., & Dwarakish, G. S. (2021). Climate change impacts on water resources in Ethiopia. *Climate Change Impacts on Water Resources: Hydraulics, Water Resources and Coastal Engineering*, 47-58.
16. Moges, D. M., & Bhat, H. G. (2021). Climate change and its implications for rainfed agriculture in Ethiopia. *journal of Water and Climate Change, 12*(4), 1229-1244.
17. Asfaw, A., Simane, B., Bantider, A., & Hassen, A. (2019). Determinants in the adoption of climate change adaptation strategies: evidence from rainfed-dependent smallholder farmers in north-central Ethiopia (Woleka sub-basin). *Environment, Development and Sustainability, 21*, 2535-2565.
18. FAO (Food and Agriculture Organization of the United Nations—with UNESCO and WMO). (1977). World map of desertification.
19. Abbate, E., & Billi, P. (2022). Geology and Geomorphological Landscapes of Eritrea. In *Landscapes and Landforms of the Horn of Africa: Eritrea, Djibouti, Somalia* (pp. 41-79). Cham: Springer International Publishing.
20. Adane, Z., Yohannes, T., & Swedenborg, E. L. (2021). Balancing water demands and increasing climate resilience: establishing a baseline water risk assessment model in Ethiopia.
21. Dorosh, P. A., & Rashid, S. (2012). Introduction [In Food and agriculture in Ethiopia: Progress and policy challenges]. *IFPRI book chapters*.
22. International Food Policy Research Institute. (2019). Global spatially-disaggregated crop production statistics data for 2010 version 2.0. *Harvard dataverse*, v4.
23. Tadele, E., & Hibistu, T. (2021). Empirical review on the use dynamics and economics of teff in Ethiopia. *Agriculture & food security, 10*, 1-13.
24. Affesse, A., Dorosh, P., & Gemessa, S. (2013). Crop production in Ethiopia: Regional patterns and trends. In P. Dorosh & S. Rashid (Eds.), Food and agriculture in Ethiopia: Progress and policy challenges (pp. 53-83). University of Pennsylvania Press.
25. Worku, M. (2019). *Quality control, quality determinants and indication of geographic origin of Ethiopian coffee* (Doctoral dissertation, PhD Thesis. Ghent University, Ghent, Belgium).
26. MoWE, F. D. R. E. (2015). Ethiopia's Climate-Resilient Green Economy. Climate Resilience Strategy: Water and Energy.
27. Adane, Z., Zlotnik, V. A., Rossman, N. R., Wang, T., & Nasta, P. (2019). Sensitivity of potential groundwater recharge to projected climate change scenarios: A site-specific study in the Nebraska Sand Hills, USA. *Water*, 11(5), 950.
28. Kishawi, Y., Mittelstet, A. R., Adane, Z., Shrestha, N., & Nasta, P. (2022). The combined impact of redcedar encroachment and climate change on water resources in the Nebraska Sand Hills. *Frontiers in Water, 4*, 1044570.
29. Spinoni, J., Vogt, J., & Barbosa, P. (2015). European degree-day climatologies and trends for the period 1951-2011. *International Journal of Climatology, 35*(1).
30. Hargreaves, G. H., & Samani, Z. A. (1985). Reference crop evapotranspiration from temperature. *Applied engineering in agriculture, 1*(2), 96-99.
31. Allen, R. G., Pereira, L. S., Raes, D., & Smith, M. (1998). Crop evapotranspiration-Guidelines for computing crop water requirements-FAO Irrigation and drainage paper 56. *Fao, Rome, 300*(9), D05109.
32. Batsukh, K., Zlotnik, V. A., Suyker, A., & Nasta, P. (2021). Prediction of biome-specific potential evapotranspiration in Mongolia under a scarcity of weather data. *Water, 13*(18), 2470.
33. Ritchie, J. T. (1972). Model for predicting evaporation from

a row crop with incomplete cover. *Water resources research, 8*(5), 1204-1213.
34. Nasta, P., & Gates, J. B. (2013). Plot-scale modeling of soil water dynamics and impacts of drought conditions beneath rainfed maize in Eastern Nebraska. *Agricultural water management, 128*, 120-130.
35. Adane, Z. A., Nasta, P., Zlotnik, V., & Wedin, D. (2018). Impact of grassland conversion to forest on groundwater recharge in the Nebraska Sand Hills. *Journal of Hydrology: Regional Studies, 15*, 171-183.
36. Šimůnek, J., Van Genuchten, M. T., & Šejna, M. (2016). Recent developments and applications of the HYDRUS computer software packages. *Vadose Zone Journal, 15*(7), vzj2016-04.
37. Van Genuchten, M. T. (1980). A closed-form equation for predicting the hydraulic conductivity of unsaturated soils. *Soil science society of America journal, 44*(5), 892-898.
38. Mualem, Y. (1976). A new model for predicting the hydraulic conductivity of unsaturated porous media. *Water resources research, 12*(3), 513-522.
39. Van Looy, K., Bouma, J., Herbst, M., Koestel, J., Minasny, B., Mishra, U., ... & Vereecken, H. (2017). Pedotransfer functions in Earth system science: Challenges and perspectives. *Reviews of Geophysics, 55*(4), 1199-1256.
40. Nasta, P., Szabó, B., & Romano, N. (2021). Evaluation of pedotransfer functions for predicting soil hydraulic properties: A voyage from regional to field scales across Europe. *Journal of Hydrology: Regional Studies, 37*, 100903.
41. Wösten, J. H. M., Lilly, A., Nemes, A., & Le Bas, C. (1999). Development and use of a database of hydraulic properties of European soils. *Geoderma, 90*(3-4), 169-185.
42. Schaap, M. G., Leij, F. J., & Van Genuchten, M. T. (2001). Rosetta: A computer program for estimating soil hydraulic parameters with hierarchical pedotransfer functions. *Journal of hydrology, 251*(3-4), 163-176.
43. Weynants, M., Vereecken, H., & Javaux, M. (2009). Revisiting Vereecken pedotransfer functions: Introducing a closed-form hydraulic model. *Vadose Zone Journal, 8*(1), 86-95.
44. Zhang, Y., & Schaap, M. G. (2019). Estimation of saturated hydraulic conductivity with pedotransfer functions: A review. *Journal of Hydrology, 575*, 1011-1030.
45. Guarracino, L. (2007). Estimation of saturated hydraulic conductivity Ks from the van Genuchten shape parameter α. *Water resources research, 43*(11).
46. Nasta, P., Vrugt, J. A., & Romano, N. (2013). Prediction of the saturated hydraulic conductivity from Brooks and Corey's water retention parameters. *Water Resources Research, 49*(5), 2918-2925.
47. Feddes, R. A. (1982). Simulation of field water use and crop yield. In *Simulation of plant growth and crop production* (pp. 194-209). Pudoc.
48. Dubache, G., Ogwang, B. A., Ongoma, V., & Towfiqul Islam, A. R. M. (2019). The effect of Indian Ocean on Ethiopian seasonal rainfall. *Meteorology and Atmospheric Physics, 131*(6), 1753-1761.
49. Lemma, W. A. (2016). Analysis of smallholder farmers' perceptions of climate change and adaptation strategies to climate change: The case of Western Amhara Region, Ethiopia. *Ethiopia Doctoral Thesis University of South Africa.*
50. Bedeke, S., Vanhove, W., Gezahegn, M., Natarajan, K., & Van Damme, P. (2019). Adoption of climate change adaptation strategies by maize-dependent smallholders in Ethiopia. *NJAS-Wageningen Journal of Life Sciences, 88*, 96-104.
51. Aboye, A. B., Kinsella, J., & Mega, T. L. (2023). Farm households' adaptive strategies in response to climate change in lowlands of southern Ethiopia. *International Journal of Climate Change Strategies and Management, 15*(5), 579-598.
52. Gebrechorkos, S. H., Hülsmann, S., & Bernhofer, C. (2019). Changes in temperature and precipitation extremes in Ethiopia, Kenya, and Tanzania. *International Journal of Climatology, 39*(1), 18-30.
53. Haile, G. G., Tang, Q., Hosseini-Moghari, S. M., Liu, X., Gebremicael, T. G., Leng, G., ... & Yun, X. (2020). Projected impacts of climate change on drought patterns over East Africa. Earth's Future, 8(7), e2020EF001502.
54. Viste, E., Korecha, D., & Sorteberg, A. (2013). Recent drought and precipitation tendencies in Ethiopia. *Theoretical and Applied Climatology, 112*, 535-551.
55. Jury, M. R. (2016). Determinants of southeast Ethiopia seasonal rainfall. *Dynamics of Atmospheres and Oceans, 76*, 63-71.
56. Gebrechorkos, S. H., Hülsmann, S., & Bernhofer, C. (2019). Regional climate projections for impact assessment studies in East Africa. *Environmental Research Letters, 14*(4), 044031.
57. Haile, G. G., Tang, Q., Hosseini-Moghari, S. M., Liu, X., Gebremicael, T. G., Leng, G., ... & Yun, X. (2020). Projected impacts of climate change on drought patterns over East Africa. *Earth's Future, 8*(7), e2020EF001502.
58. Brouwer, C., & Heibloem, M. (1986). Irrigation water management: irrigation water needs. *Training manual, 3*, 1-5.
59. Akinro, A. O., Olufayo, A. A., & Oguntunde, P. G. (2012). Crop Water Productivity of Plantain (Musa Sp) in a Humid Tropical Environment. *Journal of Engineering Science & Technology Review, 5*(1).
60. Asfew, M., & Bedemo, A. (2022). Impact of climate change on cereal crops production in Ethiopia. *Advances in Agriculture, 2022*(1), 2208694.
61. Chemura, A., Mudereri, B. T., Yalew, A. W., & Gornott, C. (2021). Climate change and specialty coffee potential in Ethiopia. *Scientific reports, 11*(1), 8097.
62. Davis, A. P., Gole, T. W., Baena, S., & Moat, J. (2012). The impact of climate change on indigenous arabica coffee (Coffea arabica): predicting future trends and identifying priorities. *PloS one, 7*(11), e47981.
63. Islam, F., Gill, R. A., Ali, B., Farooq, M. A., Xu, L., Najeeb, U., & Zhou, W. (2016). Sesame. *In Breeding Oilseed Crops for Sustainable Production* (pp. 135-147). Academic Press.
64. Hengl, T., Mendes de Jesus, J., Heuvelink, G. B., Ruiperez Gonzalez, M., Kilibarda, M., Blagotić, A., ... & Kempen, B. (2017). SoilGrids250m: Global gridded soil information based on machine learning. *PLoS one, 12*(2), e0169748.
65. Batjes, N. H., Ribeiro, E., & Van Oostrum, A. (2020).

Standardised soil profile data to support global mapping and modelling (WoSIS snapshot 2019). *Earth System Science Data, 12*(1), 299-320.

66. Poggio, L., De Sousa, L. M., Batjes, N. H., Heuvelink, G. B., Kempen, B., Ribeiro, E., & Rossiter, D. (2021). SoilGrids 2.0: producing soil information for the globe with quantified spatial uncertainty. *Soil, 7*(1), 217-240.
67. Shelia, V., Šimůnek, J., Boote, K., & Hoogenbooom, G. (2018). Coupling DSSAT and HYDRUS-1D for simulations of soil water dynamics in the soil-plant-atmosphere system. *Journal of Hydrology and Hydromechanics, 66*(2), 232-245.